

# A model for both the fast and slow spreadings of sudden events on social networks

Jiao Wu,<sup>1</sup> Muhua Zheng,<sup>2,\*</sup> Zi-Ke Zhang,<sup>3</sup> Wei Wang,<sup>4</sup> Changgui Gu,<sup>1,†</sup> and Zonghua Liu<sup>2</sup>

<sup>1</sup>Business School, University of Shanghai for Science and Technology, Shanghai 200093, China

<sup>2</sup>Department of Physics, East China Normal University, Shanghai, 200062, China

<sup>3</sup>Alibaba Research Center for Complexity Sciences, Hangzhou Normal University, Hangzhou 311121, China

<sup>4</sup>College of Computer Science and Technology, Chongqing University of Posts and Telecommunications, Chongqing 400065, China

Rumor spreading has been studied for decades, but its underlying mechanism is still under debate, especially for those ones based on internet. By focusing on the spreading data of six typical events on Sina Weibo, we surprisingly find that the spreading of modern news shows some new features, i.e. either explosively fast or slow, depending on the individual events. To understand its mechanism, we present a Susceptible-Accepted-Recovered (SAR) model with both information sensitivity and social reinforcement. By numerical simulations we show that the model can reproduce the main spreading patterns of the six typical events and the spreading speed can be promoted by increasing either the strength of information sensitivity or the social reinforcement. Moreover, we find that the dependence of final accepted size on some key parameters, such as the transmission probability and information sensitivity, can change from continuous to discontinuous when the strength of the social reinforcement is large. An edge-based theory analysis is presented to explain the explosive spreading by information sensitivity and social reinforcement.

PACS numbers: 87.23.Ge, 89.75.Hc, 05.10.-a

## I. INTRODUCTION

The spreading of information is an ubiquitous but remarkably complex phenomenon in human society and has attracted considerable interests for a long time [1–11]. This phenomenon includes the spreadings of many kinds of information on social networks, such as news [12] and rumors spreading [13, 14], innovation diffusion [15, 16], human behaviors [17–19], and culture [20, 21] etc. For the spreading of modern news, it has been revealed that the network structure plays a key role in information spreading process, especially in the aspects of spreading patterns [22, 23] and spreading threshold [24, 25]. With the increasing availability of real and good-quality data for analysis, it is now possible to study the propagation paths [26], patterns of human activities [27, 28] and the source locating [29, 30]. These results significantly increase our understanding on the mechanism of information spreading and are very useful for us to create viral marketing campaigns, block the rumor spreading, evaluate the quality of information, and predict how far it will spread.

In these studies, the complex network provides a powerful analytical framework for understanding information spreading process, where nodes are the individuals and links represent the social ties or relations among individuals [31, 32]. So far, the theoretical studies of information spreading on complex networks are mostly carried out within the framework of epidemic spreading [7, 33, 34], where the propagation takes place on links between infected and susceptible nodes. Two classical models, namely Susceptible-Infected-Susceptible (SIS) model and Susceptible-Infected-Recovered (SIR) model, are proposed to describe the traditional information spreading [35–38]. However, it has been pointed out

that the SIS and SIR models are failed to explain the empirical phenomena on real data [39] as information spreading carries its special features [40, 41]. For instance, the memory effects and social reinforcement (i.e., an individual requires multiple prompts from neighbors before adopting an opinion or behavior) [42–47] typically play an important role in the adoption of information or behavior [17]. Thus, some new models have been presented to explain the data. For examples, in Refs. [17, 18], a model taking into account the effect of social reinforcement has been presented to explain the results of Centola’s experiments on behavior spreading. In Ref.[47], with the memory effects of non-redundancy of contacts and the social reinforcement, Lü *et al* found that the small-world networks yield the most effective information spreading. More importantly, incorporating the synergistic effect to the transmission rate, the final adoption size will grow discontinuously [48–52]. In addition, the information content [5, 53] and timeliness [54] would generate various spreading patterns and paths, which are very different from epidemic spreading dynamics. It is also found that the non-redundancy of contacts [55], influential spreaders [56] and spreading channels [10] are the key ingredients in information spreading process.

Although these significant properties of information spreading have been uncovered recently, there is still not a clear picture on understanding the information spreading patterns. To take a further step to identify the drivers of information spreading, we track some spreading processes of typical events on the largest micro-blogging system in China [10]–Sina Weibo (<http://weibo.com/>). Very interestingly, we find that for the sensitive events, the information is born with fashionable features and spreads rapidly, while for the insensitive events, the information is doomed to be out of the public attentions and spreads slowly. To understand how the attribute of event influences the information spreading pattern, we adopt the sensitive intensity of information to reflect individual’s attitude towards an event (i.e., the primary accepted probability), which indicates the effect of event attribute indi-

\*Electronic address: zhengmuhua163@gmail.com

†Electronic address: gu\_changgui@163.com

rectly. Although sensitive events can apparently enhance the information spreading [39], the underlying mechanism and effect of information sensitivity is still unclear on information spreading dynamics.

A systematic study to understand the effects of information sensitivity and social reinforcement on the spreading dynamics is thus called for. In this work, we propose a model to emphasize the effect of information sensitivity on the spreading process, with the social reinforcement and the non-redundant information memory being considered. By numerical simulations we reveal that the model can show the main features of the six typical events on Sina Weibo. Increasing the strength of information sensitivity and social reinforcement can promote the information spreading. Particularly, with the increasing of information sensitivity, the spreading is faster and broader in the first stage. When the strength of the social reinforcement is large, the dependence of final accepted size on some key parameters, such as the transmission probability and information sensitivity, can be changed from continuous to discontinuous. Finally, an edge-based theory is developed, which fully explains all the numerical results.

The rest of this paper is organized as follows: In Sec. II, we describe the spreading data of six typical events on Sina Weibo. In Sec. III, we propose a new model to take into account the effects of information sensitivity and social reinforcement, and non-redundant information memory. In Sec. IV, we make numerical simulations and discuss the effects of information sensitivity and social reinforcement. In Sec. V, we give an edge-based compartmental theory to explain the numerical results. Finally, in Sec. VI, we present conclusions and discussions.

## II. DATA DESCRIPTION

To better identify the drivers of information spreading, we track some historical events spreading on the largest micro-blogging system in China [10]—Sina Weibo (<http://weibo.com/>), which evolves about 20% of the Chi-

TABLE I: Basic statistics of the six typical events. Date indicates the time of corresponding event,  $N_m(100)$  represents the cumulative number of messages talking about the corresponding event till 100 days,  $\Delta$  denotes the increasing rate of messages posted within the first 10 day.

No.	Events	Date	$N_m(100)$	$\Delta$
a	Wenzhou Train Collision	23/Jul./2011	281 905	0.9038
b	Yushu Earthquake	14/Apr./2010	24 544	0.8771
c	Death of Wang Yue	13/Oct./2011	148 297	0.7029
d	Case of Running Fast Car in Hebei University	16/Oct./2010	74 156	0.1296
e	Tang Jun Education Qualification Fake	01/Jul./2010	6776	0.2473
f	Yao Ming Retire	20/Jul./2011	45 006	0.5753

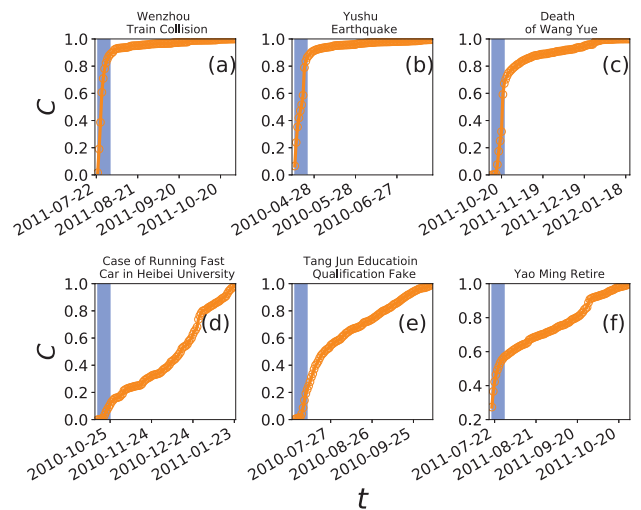


FIG. 1: (color online). The spreading dynamics versus time  $t$  for the six typical events on Sina Weibo, where (a)-(f) represent the events of Wenzhou Train Collision, Yushu Earthquake, Death of Wang Yue, Case of Running Fast Car in Hebei University, Tang Jun Education Qualification Fake, and Yao Ming Retire, respectively. Light blue areas represent the spreading range within the first 10 days of the event.

nese population. When an event occurs, individuals usually post short messages to talk about it in online social network, namely tweets in Weibo. At the same time, individuals (follower) can follow other neighbors (followers) and forward the message (i.e., retweet), which is very similar to Twitter. Therefore, Sina Weibo can efficiently reflect the spreading tendency of different events and the sensitive intensity of the event.

We collect the data in Sina Weibo from September 2009 to February 2012 and choose those events with diversity so that to represent a wide-range of topics. As a consequence, we find six typical events related to various aspects of social life, including public figures, natural disaster, traffic accident, and so on. Table I shows the basic statistics of the six typical events. The data details of these six events are as follows [10]:

(a) **Wenzhou Train Collision:** Two high-speed trains (TVG) travelling on the Yongtaiwen railway line collided at a viaduct in the suburb of Wenzhou in Zhejiang province.

(b) **Yushu Earthquake:** Yushu County, located on the Tibetan plateau in China, was awoken by a magnitude 6.9 earthquake.

(c) **Death of Wang Yue:** (also referred to as the xiao yueyue event) Wang Yue, a two year old Chinese girl, was killed in a car crash by two vehicles in a narrow street in Foshan city, Guangdong province.

(d) **Case of Running Fast Car in Hebei University:** Two students were hit by a car driven by a drunk man at a narrow lane inside the Hebei University in Hebei province.

(e) **Tang Jun Education Qualification Fake:** Tang Jun, the well-known and successful former president of Microsoft China and Shanda Interactive Entertainment, was accused by Fang Zhouzi, a crusader against scientific and academic fraud,

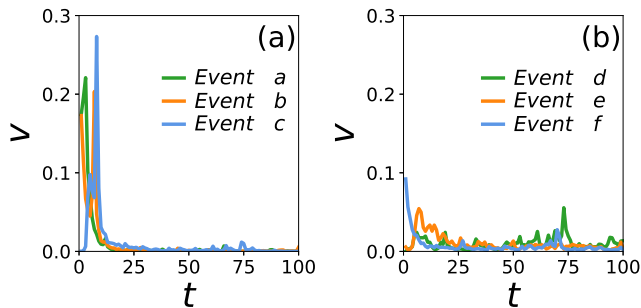


FIG. 2: (color online). (a) and (b) represent the time evolution of the spreading speed  $V$  on each day for sensitive and insensitive events, respectively.

of falsifying his academic credentials and also patents.

**(f) Yao Ming Retire:** Yao Ming officially announced his retirement from basketball after nine seasons in the team Houston Rockets.

To quantitatively describe the spreading dynamics of six selected events, we define  $C = \frac{N_m(t)}{N_m(100)}$  as the cumulative probability of messages talking about the corresponding event, where  $N_m(t)$  and  $N_m(100)$  represent the cumulative number of messages posted till time  $t$  and 100 day, respectively. It is noting that as individuals' attentions to an event decays very fast [54], we assume the information spreading process is ended after 100 days. Figs. 1 shows the spreading results of the six selected events within the first 100 day after their outbreak are different. From Figs. 1(a)-(c) we see that these three events spread rapidly in the first 10 days (shaped by Light blue), indicating that people are very sensitive to these kinds of events. Noting that Figs. 1(a)-(c) represent the events of natural disaster or traffic accident. In contrast, Fig. 1(d)-(f) represent the events which are out of public attentions and spread slowly in the first 10 days. To better characterize these different patterns, we let  $\Delta$  be the increasing rate of messages posted within the first 10 day, defined as  $\Delta = \frac{N_m(10)}{N_m(100)}$ . Then, we calculate the values of  $\Delta$  for different events. Very interestingly, we find that for the sensitive events, the information is of fashionable features and spread explosively fast within the first 10 day. While for the insensitive events, the information is dull for public attention and spreads slowly. For example, the event of Wenzhou Train Collision (Fig. 1(a)) is very attractive and its  $\Delta$  can reach 90.38% within the first 10 day. While for the event of Running Fast Car in Hebei University, it spreads slowly and its  $\Delta$  is just 12.96% within the first 10 day.

We further analyze the increment rate of messages (i.e., spreading speed) talking about the corresponding event on each day, namely  $V = \frac{C(t+\Delta t) - C(t)}{\Delta t}$ , where  $\Delta t = 1$  in our statistical process. Fig. 2 shows the time evolution of the spreading speed  $V$  for different events on each day. Comparing Fig. 2(a) with 2(b), we see that the spreading speeds  $V$  of sensitive and insensitive events are different on each day. For some sensitive events,  $V$  are larger in the first 10 days (Fig. 2(a)), indicating that the events spread rapidly. However, for

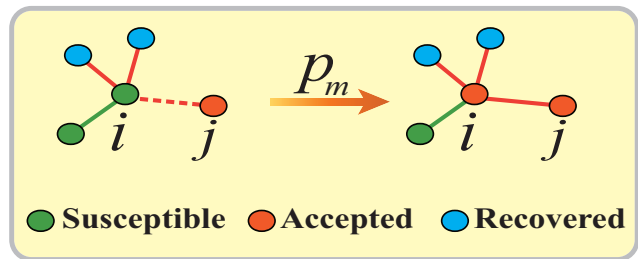


FIG. 3: (color online). Sketch of the Susceptible-Accepted-Recovered (SAR) model on complex networks, where the red solid line denotes that the information has been transmitted successfully through it previously. At time  $t$ , the susceptible node  $i$  may receive the information about an event from an accepted node  $j$  with probability  $\beta$  (marked with a red dashed line). Once node  $i$  receives the information successfully from the neighbor  $j$ , the cumulative number  $m$  of received information will increase 1 for node  $i$ . Assuming that node  $i$  has received a new piece of information from  $j$  at time  $t$ , the cumulative number  $m$  will be 3 in this example and node  $j$  will not transmit the same information to node  $i$  any more. Then the accepted probability will be given by Eq. (2).

the insensitive ones, their  $V$  are smaller than the cases of Fig. 2(a), implying that the events spread slowly. That is, both the explosive and dilatory spreading are general at the early stage of information spreading. Then, a key question is, what are their underlying mechanisms.

### III. A MODEL FOR THE SPREADING OF SOCIAL EVENTS

To reproduce the spreading patterns of real data, we introduce a model of information spreading on complex networks. We consider an uncorrelated network with  $N$  nodes,  $E$  links and degree distribution  $P(k)$ , where nodes represent individuals of population and the spreading process occurs only between the neighboring nodes through links. Fig. 3 shows the schematic figure of the model. At each time step, a node can take only one of the three states: (i) Susceptible: the node has not received information on event yet or has received information but hesitate to accept it; (ii) Accepted: the node accepts the information and transmits it to the neighbors; (iii) Recovered: the node loses interest to the information and will not spread the information any more. Thus, this Susceptible-Accepted-Recovered (SAR) model is similar to the SIR model in epidemiology.

The information spreading process can be described as follows:

(i) To initiate an event, a fraction  $\rho_0$  of nodes are random uniformly chosen from the considered network as seeds (accepted state) to spread the first piece of information. All other nodes are in the susceptible state.

(ii) At each time step  $t$ , every accepted node will post the information and propagate it to each of its neighbors independently, with a transmission probability  $\beta$ . Once the transmission is successfully reached a neighbor, the cumulative number  $m$  of received information will be increased by one for this

neighbor. In our model, as people rarely transmit the same information to one person once and once again, an edge that has transmitted the information successfully will never transmit the same information again, i.e., non-redundant information transmission.

(iii) At a time step  $t$ , the probability for a susceptible node to accept an information is  $p_m$  (see Eq. (2)) if it receives the information at least once at the  $t$ -th time step and has received it  $m$  times until time  $t$ . At the same time step, each accepted node will lose interest in transmitting the information and becomes recovered with probability  $\mu$ .

(iv) The steps are repeated until all accepted nodes have become recovered.

Now, the key point is how to define the accepted probability  $p_m$ . Inspired by our previous work in Ref [18], we adopt the accepted probability  $p_m$  as follows. When a node receives the information at the first time, it will accept the information with probability  $p_1 = \lambda$ , where  $\lambda$  is the information sensitivity reflecting the sensitive intensity of information for an event. Larger  $\lambda$  means that the information is more sensitive and individuals are likely to accept the information. When a node receives the information twice or three times, it will accept the information with a probability  $p_2$  or  $p_3$ , respectively. In our model, the accepted probability with different received times is defined as following:

$$\begin{aligned} p_1 &= \lambda, \\ p_2 &= p_1 + \eta \times (1 - p_1), \\ p_3 &= p_2 + \eta \times (1 - p_2), \\ &\vdots \\ p_m &= p_{m-1} + \eta \times (1 - p_{m-1}), \end{aligned} \quad (1)$$

where  $\eta \in [0, 1]$  is the social reinforcement strength. Larger  $\eta$  means that redundant information will have stronger influence on nodes. The iterative Eq. (1) indicates that if the node has received the information  $m$  times, the approving probability will increase  $\eta \times (1 - p_{m-1})$ , comparing with  $p_{m-1}$ . The increase can be considered as an increment of spreading rate converted from disapproving probability  $1 - p_{m-1}$  under the effect of social reinforcement. In sum, the Eqs. (1) can be simplified into

$$p_m = 1 - (1 - \lambda)(1 - \eta)^{m-1}, 0 \leq \eta \leq 1, m \geq 1. \quad (2)$$

It is found that by Eq. (2), the simulation results can well explain the results of Centola's experiments on behavior spreading and some former studies on information spreading in different parameter spaces [17, 18]. It is worth noting that our model has three key parameters: the transmission probability  $\beta$ , the information sensitivity  $\lambda$  and the social reinforcement strength  $\eta$ . This model emphasizes the effect of the information sensitivity, social reinforcement and non-redundant information memory, which make the information spreading processes be non-Markovian.

## IV. RESULTS

### A. Reproduce the spreading patterns of six typical events in Sina Weibo

In numerical simulations, we adopt the Erdős-Rényi (ER) random network to study the information spreading process, with the network size  $N = 10\,000$  and the average degree  $\langle k \rangle = 6$ . At the same time, we let  $\rho_0 = 0.01$  and  $\mu = 1.0$  in this paper.

For better comparison with empirical analyses, we let  $\rho_R(t)$  denote the fraction of recovered nodes at time  $t$  in the information spreading process. Fig. 4(a) shows the evolution of  $\rho_R$  with different information sensitivity  $\lambda$ . It is easy to observe that the model can somehow show the main spreading patterns of real Weibo data. Particularly, the spreading pattern is similar to the cases of Figs. 1(d)-(f) when  $\eta = 0.4$  and information sensitivity  $\lambda$  is relatively small, where the information spreads slowly in the first 10 time steps (see the light blue shadowed areas). However,  $\rho_R$  will increase sharply in the first 10 time steps and shows the same pattern as the cases of Figs. 1(a)-(c) (see the light blue shadowed areas) when  $\lambda$  is large. Another important parameter is the spreading speed. Here, we redefine  $V = \frac{\rho_R(t+\Delta t) - \rho_R(t)}{\Delta t}$  and set  $\Delta t = 1$  as the empirical analyses. A larger  $V$  indicates a faster spreading speed at time  $t$ . The spreading process will be ended when  $V = 0$ , where the spreading range will reach its maximum. Fig. 4(c) shows the evolution of  $V$ , corresponding to Fig. 2(a). It is easy to see that the peak of  $V$  is mainly located in the first 10 time steps when  $\lambda$  is large, indicating that the information spreads rapidly in the early stage. These results are consistent with the empirical observations in Fig. 2(a). However, when information sensitivity is small (i.e.,  $\lambda = 0.2$ ),  $V$  will be smaller than the case of large  $\lambda$ , which indicates that the spreading of information is slowly in the early stage. The peak of  $V$  also falls behind in the time domain, indicating that the occurrence of outbreak has been delayed. These findings are consistent with the empirical phenomena in Fig. 2(b). Thus, it can be concluded that the model can show the main features of real data of Sina Weibo. At the same time, these results reveal that the information sensitivity  $\lambda$  has a strong influence in the early stage of spreading process.

Another important problem is how the social reinforcement influences the range and speed of information spreading. To answer this problem, we plot the time evolution of the fraction of recovered nodes  $\rho_R$  with fixed  $\lambda = 0.4$  in Fig. 4(b). It is easy to observe that the difference of spreading range with different  $\eta$  is insensitive for  $t < 8$ . After that, with the increasing of social reinforcement  $\eta$ , the spreading range is becoming more and more broader, implying that the influence of social reinforcement mainly contributes on the following stage. In this stage, an individual has more chances to receive multiple information in that the accepted probability is increased by the social reinforcement. More importantly, as is shown in Fig. 4(d), a larger social reinforcement  $\eta$  will also accelerate the information spread, indicating that the social reinforcement is another key ingredient in information spreading process.

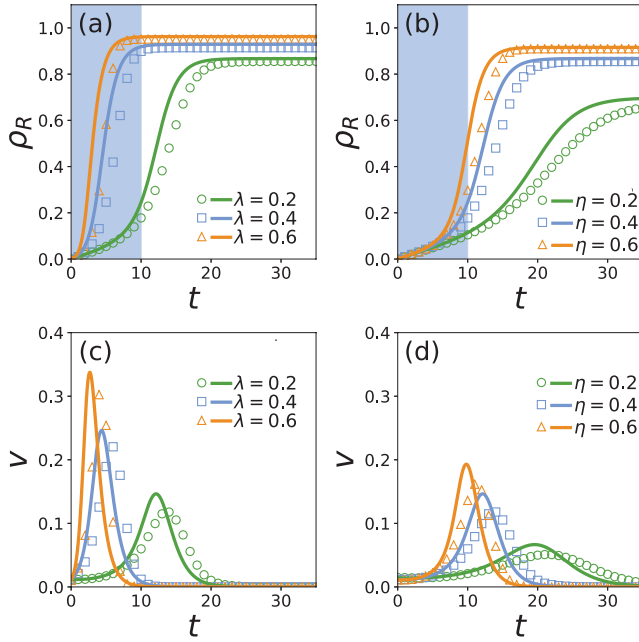


FIG. 4: (color online). (a) and (b) represent the fraction of recovered nodes  $\rho_R$  as a function of time  $t$  with different information sensitivity  $\lambda$  and different social reinforcement  $\eta$ , respectively. Light blue areas represent the spreading range within 10 time steps in the spreading process. (c) and (d) represent the information spreading speed  $V$  as a function of time  $t$  corresponding to (a) and (b), respectively. Symbols represent the simulated results and the lines are the corresponding theoretical results. The parameters are fixed as  $\eta = 0.4$  in (a)(c) and  $\lambda = 0.4$  in (b)(d), respectively. Other parameters are set as  $N = 10\,000$ ,  $\beta = 0.8$ ,  $\rho_0 = 0.01$ ,  $\mu = 1.0$ . All the results are averaged over 100 independent realizations.

### B. Effects of dynamical parameters

To quantitatively represent the effects of  $\lambda$  and  $\eta$  in the early stage [10], we here measure the increasing rate  $\Delta$  of recovered nodes within the first 10 time steps (i.e., the density of recovered nodes at  $t = 10$ ). Figs. 5(a) and (b) show the increasing rate  $\Delta$  of recovered nodes as a function of information sensitivity  $\lambda$  in ER network with different  $\eta$  and  $\beta$ , respectively. As is show in Fig. 5(a),  $\Delta$  increases gradually with  $\lambda$  for a fixed  $\eta$ . A larger  $\eta$  will promote the increase of  $\Delta$  sharply, indicating that both information sensitivity  $\lambda$  and social reinforcement  $\eta$  will increase the value of  $\Delta$  and accelerate the information spreading. Very interesting, we find that the transmission probability  $\beta$  also plays a key role on  $\Delta$ . As is shown in Fig. 5(b),  $\Delta$  increase slowly when  $\beta$  is small, indicating that information is difficult to spread out. Once  $\beta$  is relatively large, a larger  $\lambda$  or  $\eta$  will make the information spread fast. As a larger  $\beta$  will make a node to receive the information easily from its neighbors, the redundant information will increase the accepted probability  $p_m$  and result in the fast information spreading.

A key quantity of spreading dynamics is the final size of accepted nodes, denoted by  $\rho_R(\infty)$ . Larger  $\rho_R(\infty)$  at the final state indicates broader spreading. Fig. 6(a) shows the final ac-

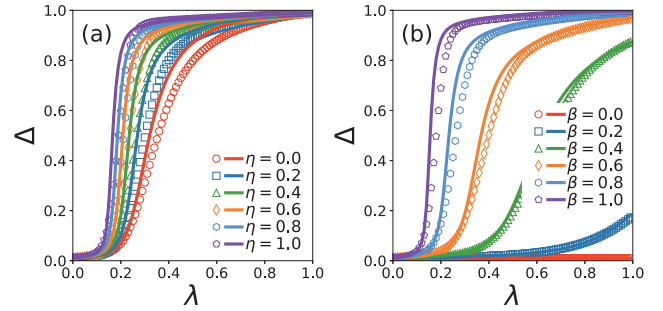


FIG. 5: (color online). (a) and (b) represent the increasing rate  $\Delta$  of recovered nodes within the first 10 time steps, as a function of information sensitivity  $\lambda$  in ER network with different  $\eta$  and  $\beta$ , respectively. Symbols represent the simulated results and the lines are the corresponding theoretical results. The parameters are fixed as  $\beta = 0.8$  in (a) and  $\eta = 0.4$  in (b), respectively. Other parameters are the same as in Fig. 4.

cepted size  $\rho_R(\infty)$  versus information sensitivity  $\lambda$  for different  $\eta$ . We see that for a small social reinforcement  $\eta$ ,  $\rho_R(\infty)$  increases continuously with  $\lambda$ . However, for a slightly larger social reinforcement (i.e.,  $\eta = 0.4$ ), the pattern of  $\rho_R(\infty)$  versus  $\lambda$  becomes discontinuous, exhibiting an abrupt increase at the critical value  $\lambda_c$ . When  $\lambda < \lambda_c$ , the information will not be spread out. While  $\lambda > \lambda_c$ , the information will be spread out explosively. As a small  $\eta$  will reduce the accepted probability  $p_m$ , a node will not accept the information until it receives the information multiple times (i.e.,  $m$  should be large). As a result, nodes are not likely to accept the information and the spreading range  $\rho_R(\infty)$  will be narrow when the social reinforcement  $\eta$  is relatively small. Besides the social reinforcement  $\eta$ , the information transmission rate  $\beta$  also has strong influence on the final accepted size  $\rho_R(\infty)$ . Fig. 6(b) shows  $\rho_R(\infty)$  versus information sensitivity  $\lambda$  for different  $\beta$ . It is easy to observe that when  $\beta = 0$ , the information can not be spread out, no matter how large the  $\lambda$  is. This is a trivial case as individuals can not receive any information. Once  $\beta$  is larger (i.e.,  $\beta = 0.2$ ),  $\rho_R(\infty)$  increases continuously with  $\lambda$ . However, for a very larger transmission probability (i.e.,  $\beta = 0.6$ ), the increasing of  $\rho_R(\infty)$  with  $\lambda$  becomes discontinuous, exhibiting an explosive phase transition at the critical value  $\lambda_c$ . As a large transmission probability is preferred to receive the information for individuals, it promotes the information spreading.

It is well known that there is a critical  $\beta_c$  in epidemic spreading, although it may be different for different cases. In the thermodynamic limit, the infected fraction will be zero when  $\beta < \beta_c$ , and it will become nonzero at  $\beta = \beta_c$ . After the critical point  $\beta_c$ , the infected fraction will gradually increase with a further increase of  $\beta$ . Similarly, in this work, we are also interested in the effects of transmission probability  $\beta$  on  $\rho_R(\infty)$  with different  $\lambda$  and  $\eta$ . Fig. 6(c) and (d) show the dependence of  $\rho_R(\infty)$  on the transmission probability  $\beta$  with different  $\lambda$  and  $\eta$ , respectively. From Fig. 6(c), we have  $\rho_R(\infty) = 0$  when  $\lambda = 0$ , indicating that no one have interesting to spread this information. However, in the nontrivial

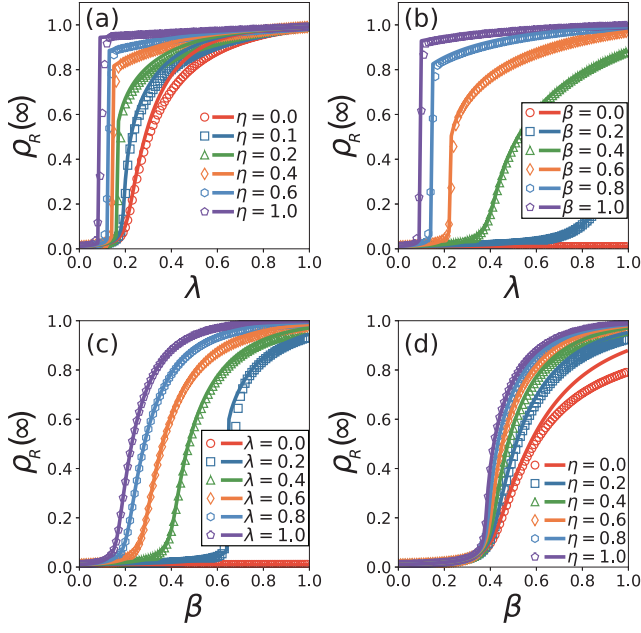


FIG. 6: (color online). Final states of information spreading dynamics on ER networks. The final accepted size  $\rho_R(\infty)$  versus information sensitivity  $\lambda$  with (a) different  $\eta$  and (b) different  $\beta$ . (c) and (d) report the dependence of  $\rho_R(\infty)$  on transmission probability  $\beta$  with different  $\lambda$  and  $\eta$ , respectively. Symbols represent the simulated results and the lines are the corresponding theoretical results. The parameters are fixed as (a)  $\beta = 0.8$ , (b)  $\eta = 0.4$ , (c)  $\eta = 0.4$  and (d)  $\lambda = 0.4$ , respectively. Other parameters are the same as in Fig. 4.

case of  $\lambda > 0$ , it is visible to observe that there is a critical point  $\beta_c$ . When  $\beta < \beta_c$ , we have  $\rho_R(\infty) = 0$ , indicating that the information can not be spread out. Once  $\beta > \beta_c$ ,  $\rho_R(\infty)$  will increase gradually with  $\beta$ . More importantly, the  $\beta_c$  will decrease with the increase of  $\lambda$ , implying that a large  $\lambda$  will promote the information spreading. However, for different  $\eta$ , the situation is different with  $\lambda$ . Although large  $\eta$  will increase  $\rho_R(\infty)$  for large  $\beta$ , the critical value  $\beta_c$  is insensitive with the increase of  $\eta$  (see Fig. 6(d)). As the node is unlikely to receive the information multiple times in early stage, the contribution of social reinforcement becomes non-significant on  $\rho_R(\infty)$  in this stage, leading to that  $\beta_c$  is insensitive on  $\rho_R(\infty)$ . From these analyses, it can be concluded that  $\beta$ ,  $\lambda$  and  $\eta$  markedly affect  $\rho_R(\infty)$  and phase transition. To gain further insights into the critical phenomenon, we will investigate the phase transition on a different parameter plane in the next section.

## V. A THEORETICAL ANALYSIS BASED ON EDGE-BASED COMPARTMENTAL THEORY

We now give a theoretical analysis to explain the information spreading patterns of the proposed model. We first apply the edge-based compartmental theory on complex networks, by following the methods and tools introduced in Refs. [24, 25, 57–63].

For an uncorrelated, large and sparse network, the proposed model can be described in terms of the quantities:  $\rho_S(t)$ ,  $\rho_A(t)$ , and  $\rho_R(t)$ , which are the densities of the Susceptible, Accepted, and Recovered nodes at time  $t$ , respectively. When  $t \rightarrow \infty$ , the spreading process is ended and  $\rho_R(\infty)$  represent the final fraction of nodes that have accepted the information.

Now, we use a variable  $\theta(t)$  to denote the probability that a node  $v$  has not transmitted the information to node  $u$  along a randomly chosen edge by time  $t$ . Then, the probability that a randomly chosen node  $u$  of degree  $k$  has received the information from distinct neighbors  $m$  times at time  $t$  is

$$\phi_m(k, \theta(t)) = \binom{k}{m} \theta(t)^{k-m} [1 - \theta(t)]^m. \quad (3)$$

Clearly, the node with degree  $k$  has the probability  $1 - \rho_0$  to be not one of the initial seeds. The probability that an arbitrary node has not accepted the information after receiving such information  $m$  times is  $\prod_{j=1}^m (1 - p_j) = (1 - \lambda)^{\sum_{j=1}^m j} (1 - \eta)^{\sum_{j=1}^m j-1}$ . Then, we can derive the probability that a susceptible node  $u$  with degree  $k$  has received the information  $m$  times and still does not accept it by time  $t$  as  $\phi_m(k, \theta(t)) (1 - \lambda)^{\sum_{j=1}^m j} (1 - \eta)^{\sum_{j=1}^m j-1}$ . Combining the initial seeds and summing over all possible values of  $m$ , we obtain the probability that the node  $u$  is still in the susceptible state at time  $t$  as

$$S(k, t) = (1 - \rho_0) \sum_{m=0}^k \phi_m(k, \theta(t)) \times (1 - \lambda)^{\sum_{j=1}^m j} (1 - \eta)^{\sum_{j=1}^m j-1}. \quad (4)$$

Averaging over all  $k$ , the density of susceptible nodes (i.e., the probability of a randomly chosen individual is in the susceptible state) at time  $t$  is given by

$$\rho_S(t) = \sum_{k=0}^{\infty} P(k) S(k, t). \quad (5)$$

Since a neighbor  $v$  of node  $u$  may be susceptible, infected, or recovered,  $\theta(t)$  can be expressed as

$$\theta(t) = \Phi^S(t) + \Phi^A(t) + \Phi^R(t). \quad (6)$$

where  $\Phi^S(t)$ ,  $\Phi^A(t)$ ,  $\Phi^R(t)$  is the probability that the neighbor  $v$  is in the susceptible, accepted, recovery state, respectively, and has not transmitted the information to node  $u$  through their connections. Once these three parameters can be derived, we will get the density of susceptible nodes at time  $t$  by substituting them into Eq. (4) and then into Eq. (5). To this purpose, in the following, we will focus on how to solve them.

To find  $\Phi^S(t)$ , we consider a randomly selected node  $u$  with degree  $k$ , and assume that this node is in the cavity state [40,43], which means that it cannot transmit any information to its neighbors  $v$  but can receive such information from its neighbors. In this case, the neighbor  $v$  can only get the information from its other neighbors except the node  $u$ . So, if

a neighboring node  $v$  of  $u$  has degree  $k'$ , the probability that node  $v$  has received  $m$  pieces of the information at time  $t$  is

$$\psi_m(k', \theta(t)) = \binom{k'-1}{m} \theta(t)^{k'-m-1} [1 - \theta(t)]^m. \quad (7)$$

Similar to Eq. (4), individual  $v$  will still stay in the susceptible state by time  $t$  with the probability

$$\Theta(k', \theta(t)) = (1 - \rho_0) \sum_{m=0}^{k'-1} \psi_m(k', \theta(t)) \times (1 - \lambda)^{\sum_{j=1}^m j} (1 - \eta)^{\sum_{j=1}^m j-1}. \quad (8)$$

For uncorrelated networks, the probability that one edge from node  $u$  connects with a node with degree  $k'$  is  $k'P(k')/\langle k \rangle$ , where  $\langle k \rangle$  is the mean degree of the network. Summing over all possible  $k'$ , we obtain the probability that  $u$  connects to a susceptible node by time  $t$  as

$$\Phi_S(t) = \frac{\sum_{k'} k' P(k') \Theta(k', \theta(t))}{\langle k \rangle}. \quad (9)$$

According to the information spreading process as described in Sec.II, the growth of  $\Phi^R(t)$  includes two consecutive events: first, an accepted neighbor has not transmitted the information successfully to node  $u$  with probability  $1 - \beta$ ; second, the accepted neighbor has been recovered with probability  $\mu$ . Combining these two events, the  $\Phi^I(t)$  to  $\Phi^R(t)$  flux is  $\mu(1 - \beta)\Phi^I(t)$ . Thus, one gets

$$\frac{d\Phi^R(t)}{dt} = \mu(1 - \beta)\Phi^A(t). \quad (10)$$

Once the accepted neighbor  $v$  transmits the information to  $u$  successfully (with probability  $\beta$ ), the  $\Phi^A(t)$  to  $1 - \theta(t)$  flux will be  $\beta\Phi^A(t)$ , which means

$$\frac{d(1 - \theta(t))}{dt} = \beta\Phi^A(t),$$

That is

$$\frac{d\theta(t)}{dt} = -\beta\Phi^A(t). \quad (11)$$

Combining Eqs. (10) and (11), and considering (as initial conditions)  $\theta(0) = 1$  and  $\Phi^R(0) = 0$ , one obtains

$$\Phi_R(t) = \frac{\mu[1 - \theta(t)](1 - \beta)}{\beta}. \quad (12)$$

Substituting Eqs. (9) and (12) into Eq.(6), we get an expression for  $\Phi^A(t)$  in terms of  $\theta(t)$ , and then one can rewrite Eq. (11) as

$$\frac{d\theta(t)}{dt} = -\beta \left[ \theta(t) - \frac{\sum_{k'} k' P(k') \Theta(k', \theta(t))}{\langle k \rangle} \right] + \mu[1 - \theta(t)](1 - \beta). \quad (13)$$

With  $\theta(t)$  on hand, the equation of the system comes out to be

$$\begin{aligned} \frac{d\rho_R(t)}{dt} &= \mu\rho_A(t), \\ \rho_S(t) &= \sum_{k=0}^{\infty} P(k)S(k, t), \\ \rho_A(t) &= 1 - \rho_S(t) - \rho_R(t) \end{aligned} \quad (14)$$

Eqs. (14) give us the densities for each type of nodes in each state at arbitrary time step and are the main theoretical results from which the theoretical curves in Figs. 4 and 5 are calculated.

Furthermore, we can obtain the final accepted size  $\rho_R(\infty)$  in the steady state (i.e., the final fraction of nodes that have accepted the information). By setting  $t \rightarrow \infty$  and  $\frac{d\theta(t)}{dt} = 0$  in Eq.(13), we get

$$\begin{aligned} \theta(\infty) &= \frac{\sum_{k'} k' P(k') \Theta(k', \theta(\infty))}{\langle k \rangle} \\ &+ \frac{\mu[1 - \theta(\infty)](1 - \beta)}{\beta}. \end{aligned} \quad (15)$$

Substituting  $\theta(\infty)$  into Eqs.(3)–(5), we can calculate the value of  $\rho_S(\infty)$ , and then the final accepted size can be obtained as

$$\rho_R(\infty) = 1 - \rho_S(\infty). \quad (16)$$

According to Eqs. (16), we obtain the theoretical results in Fig. 6, which are consistent with the numerical results.

Similar to analyzing epidemic spreading, we can obtain the critical condition where a nontrivial solution of Eq. (15) appears, which corresponds to the point at which the equation

$$\begin{aligned} g[\theta(\infty)] &= \frac{\sum_{k'} k' P(k') \Theta(k', \theta(\infty))}{\langle k \rangle} \\ &+ \frac{\mu[1 - \theta(\infty)](1 - \beta)}{\beta} - \theta(\infty). \end{aligned} \quad (17)$$

is tangent to horizontal axis at the critical value of  $\theta_c(\infty)$ . The value of  $\theta_c(\infty)$  denotes the critical probability that the information is not transmitted to  $u$  via an edge at the critical transmission probability when  $t \rightarrow \infty$ . So we obtain the critical condition of the proposed model as

$$\left. \frac{dg[\theta(\infty)]}{d\theta(\infty)} \right|_{\theta_c(\infty)} = 0. \quad (18)$$

That is

$$\frac{\sum_{k'} k' P(k) \frac{d\Theta(k', \theta(\infty))}{d\theta(\infty)} \big|_{\theta_c(\infty)}}{\langle k \rangle} - \frac{\mu(1 - \beta)}{\beta} - 1 = 0 \quad (19)$$

where

$$\begin{aligned} \frac{d\Theta(k', \theta(\infty))}{d\theta(\infty)} &= (1 - \rho_0) \sum_{m=0}^{k'-1} \binom{k'-1}{m} \\ &\times \left\{ (k' - m - 1)\theta(\infty)^{k'-m-2}[1 - \theta(\infty)]^m \right. \\ &\quad \left. - m\theta(\infty)^{k'-m-1}[1 - \theta(\infty)]^{m-1} \right\} \\ &\times (1 - \lambda)^{\sum_{j=1}^m j} (1 - \eta)^{\sum_{j=1}^m j-1}. \end{aligned} \quad (20)$$

From Eq. (18), we can calculate the critical transmission probability:

$$\beta_c = \frac{\mu}{\mathcal{A} + \mu - 1}, \quad (21)$$

where

$$\mathcal{A} = \frac{\sum_{k'} k' P(k') \frac{d\Theta(k', \theta(\infty))}{d\theta(\infty)} |_{\theta_c(\infty)}}{\langle k \rangle}. \quad (22)$$

Numerically solving Eqs. (15) and (21)–(22), we can get the critical value of the transmission probability  $\beta_c$  for any given  $\lambda$  and  $\eta$ . Similarly, for any given  $\beta$  and  $\eta$ , we can obtain the critical value  $\lambda_c$  by numerically solving Eqs. (15) and (18).

Now, a key question is to find out whether the dependence of the final accepted size  $\rho_R(\infty)$  on the transmission probability  $\beta$  and information sensitivity  $\lambda$  is continuous or discontinuous. As shown in Fig. 7, numerical calculations indicate that the number of roots in Eq. (15) is either one or three for given parameters. From Fig. 7(a), we find that the number of roots of Eq. (15) depends on  $\lambda$  for given other parameters. If Eq. (15) has only one root,  $\rho_R(\infty)$  increases continuously with  $\lambda$  [24]. When Eq. (15) has three roots, it means that a saddle-node bifurcation will occur, which indicates that the system undergoes a cusp catastrophe [24, 64]:  $\rho_R(\infty)$  increases discontinuously with  $\lambda$  (see Fig. 4(a)). As the nodes in the accepted state persistently transmit the information to their neighbors,  $\theta(t)$  decreases with  $t$ . If more than one stable fixed point exists in Eq. (15), only the maximum one is physically meaningful [24]. The tangent point that is marked as red circle is the physically meaningful solution at critical  $\lambda_c$  (e.g.,  $\lambda_c = 0.136$ ). For  $\lambda > \lambda_c$  (e.g.,  $\lambda = 0.15$ ), the solution of Eq. (15) changes to a smaller solution abruptly, which leads to a discontinuous change in  $\rho_R(\infty)$ . We can demonstrate the type of dependence and obtain the value of  $\beta_c$  for other parameters through the similar measure (as is show in Fig. 7(b)).

Finally, to determine the value of critical parameter  $\theta_s(\infty)$  where the dependence of  $\rho_R(\infty)$  on  $\lambda$  and  $\beta$  will change from continuous (discontinuous) to discontinuous (continuous), we can numerically solve Eqs. (15) and (18) together with the condition

$$\frac{d^2 g[\theta(\infty)]}{d\theta^2(\infty)} = \frac{\sum_{k'} k' P(k') \frac{d^2 \Theta(k', \theta(\infty))}{d\theta^2(\infty)} |_{\theta_c(\infty)}}{\langle k \rangle} = 0 \quad (23)$$

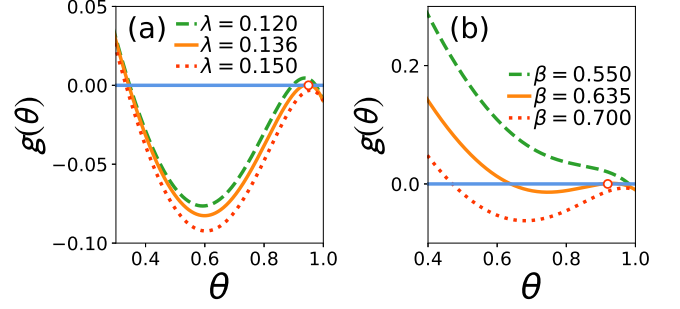


FIG. 7: (color online). Illustration of graphical solutions of Eq. (15). (a)  $\beta = 0.8$ ,  $\eta = 0.4$ , (b)  $\lambda = 0.4$ ,  $\eta = 0.4$ . The blue solid line is the horizontal axis and the red circle denotes the tangent point. The parameters for the simulations are  $N = 10\,000$ ,  $\langle k \rangle = 6$ ,  $\rho_0 = 0.01$ ,  $\mu = 1.0$ .

Using Eq. (20), we get

$$\begin{aligned} \frac{d^2 \Theta^2(k', \theta(\infty))}{d\theta^2(\infty)} &= (1 - \rho_0) \sum_{m=0}^{k'-1} \binom{k'-1}{m} (\mathcal{F} + \mathcal{G} + \mathcal{M} + \mathcal{N}) \\ &\times (1 - \lambda)^{\sum_{j=1}^m j} (1 - \eta)^{\sum_{j=1}^m j-1}, \end{aligned} \quad (24)$$

where

$$\begin{aligned} \mathcal{F} &= (k' - m - 1)(k' - m - 2)\theta(\infty)^{k'-m-3}[1 - \theta(\infty)]^m \\ \mathcal{G} &= -m(k' - m - 1)\theta(\infty)^{k'-m-2}[1 - \theta(\infty)]^{m-1} \\ \mathcal{M} &= m(m - 1)[1 - \theta(\infty)]^{m-2}\theta(\infty)^{k'-m-1} \\ \mathcal{N} &= -m(k' - m - 1)\theta(\infty)^{k'-m-2}[1 - \theta(\infty)]^{m-1} \end{aligned} \quad (25)$$

Combining Eqs. (15), (18) and (24), we get the value of  $\theta_s(\infty)$ . For fixed  $P(k)$ , the critical values of other system parameters, e.g.,  $\lambda_s$  and  $\beta_s$ , can then be determined. In Fig. 8(a) and (b), we plot the phase diagram of the final accepted size  $\rho_R(\infty)$  on parameter space  $(\lambda, \eta)$  and  $(\beta, \lambda)$ , respectively. From Fig. 8(a), we find that for fixed  $\beta = 0.8$ , when the social reinforcement  $\eta$  is large,  $\rho_R(\infty)$  increase with  $\lambda$  discontinuously (i.e., region I). Moreover, the critical value  $\lambda_c$  will decrease with the increasing of  $\eta$  (white circles in Fig. 8(a)). When  $\eta$  is small, our model is similar to SIR model in epidemiology [18]. In this case, the dependence of  $\rho_R(\infty)$  on  $\lambda$  is continuous (i.e., region II), which is consistent with the former results [7]. Region I and II are separated by the vertical green dashed lines, which are predicted by  $\lambda_s$  from Eqs. (15), (18) and (24).

From Fig. 8(b), we observe that a crossover phenomenon occurs in the dependence of  $\rho_R(\infty)$  on  $\beta$ . The crossover phenomenon means that the dependence of  $\rho_R(\infty)$  on  $\beta$  can change from continuous to discontinuous. The crossover point  $\beta_s$ , as indicated by the vertical green dashed line, can be calculated analytically by solving Eqs. (15), (18) and (24). More specifically, the saddle-node bifurcation of Eq. (15) occurs for  $\beta_c > 0.57$  (region I in Fig. 8(b)), thus  $\rho_R(\infty)$  versus  $\beta$  is discontinuous. However,  $\rho_R(\infty)$  versus  $\beta$  is continuous for

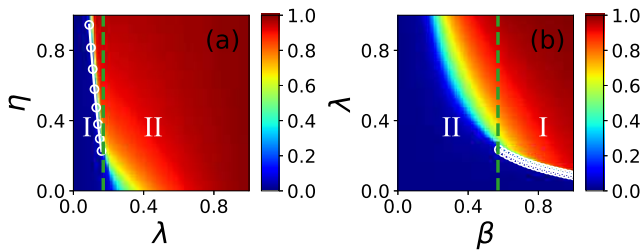


FIG. 8: (color online). Phase diagram of the final accepted size. (a) represents the dependence of  $\rho_R(\infty)$  on  $\lambda$  and  $\eta$  with  $\beta = 0.8$ . (b) represents the dependence of  $\rho_R(\infty)$  on  $\beta$  and  $\lambda$  with  $\eta = 0.4$ . Color-coded represent the values of  $\rho_R(\infty)$  from numerical simulations. The critical values of  $\lambda_c$  and  $\beta_c$  (white circles) are from Eqs. (15) and (18)-(21). The vertical green dash lines separate the plane into the two regions, which are predicted from Eqs. (15), (18), and (24). Region I shows that  $\rho_R(\infty)$  grows discontinuously with  $\lambda$  and  $\beta$  in (a) and (b), respectively.  $\rho_R(\infty)$  grows continuously to a large value in region II. All the numerical results are averaged over 1000 independent realizations. Other parameters are set as Fig. 4.

$\beta < 0.57$  (region II in Fig. 8(b)), as the saddle-node bifurcation disappears. More importantly, the  $\beta_c$  will decrease with the increasing of  $\lambda$ , meaning that a large  $\lambda$  will promote the information spreading. The theoretically predicted behaviors of  $\rho_R(\infty)$  is well consistent with numerical simulations.

## VI. DISCUSSION

The study of information spreading in social networks is an extremely challenging problem. In the recent years, with the fast development of database technology and computational power, detailed analysis of information spreading in large-scale online systems has become feasible. In this work, by analyzing a large database of Sina Weibo, we show that for the sensitive events, the information is born with fashionable features and spread explosively fast, while for the insensitive

events, the information is doomed to be out of the public attention and spreads slowly. In order to understand how information transmits on peer-to-peer interactions, we present a SAR model to represent the information spreading on social networks, which includes three essential properties of the information spreading: (i) information sensitivity; (ii) social reinforcement; and (iii) non-redundant information memory. By both numerical simulations and theoretical analysis we show that the information spreading can be either explosively fast or very slow, which agrees well with empirical data. Further, we reveal that the information spreading can be promoted by increasing either the strength of information sensitivity or social reinforcement. Especially, with the increasing of information sensitivity, the spreading is faster and broader in the first stage. When the strength of the social reinforcement is large, the final accepted size will increase explosively with the transmission probability and information sensitivity. These findings may provide an explanation for the extremely fast spreading of modern fashion such as the news, rumours and products etc.

The main contributions of this work are thus the discovery of explosive and dilatory spreading patterns from the data of Sina Weibo, and a qualitative and quantitative understanding of the phenomenon by the SAR model. However, many challenges still remain. For example, more real data of information spreading are needed to further test the validity of the model. Moreover, the effects of network structural characteristics such as degree heterogeneity [32], clustering [65, 66], community [67–69], and core periphery [70–73] on information spreading need to be studied. Finally, the study needs to be extended to more realistic networks such as multi-layer networks [74–76], temporal networks [77] and so on.

This work was partially supported by the NNSF of China under Grant Nos. 11505114, 11375066 and 11675056, 973 Program under Grant No. 2013CB834100, and the Program for Professor of Special Appointment (Oriental Scholar) at Shanghai Institutions of Higher Learning under Grants No. QD201.

- 
- [1] W. Gofman, and V. A. Newill, *Nature* **204**, 225C228 (1964).  
[2] D. J. Daley, and D. G. Kendall, *Nature* **204**, 1118 (1964).  
[3] H. P. Young, *Proc. Natl. Acad. Sci. USA* **108**, 21285 (2011).  
[4] J. Ratkiewicz, S. Fortunato, A. Flammini, F. Menczer, and A. Vespignani, *Phys. Rev. Lett.* **105**, 158701 (2010).  
[5] R. Crane, and D. Sornette, *Proc. Natl. Acad. Sci. USA* **105**, 15649 (2008).  
[6] D. Sornette, F. Deschates, T. Gilbert, and Y. Ageon, *Phys. Rev. Lett.* **93**, 228701 (2004).  
[7] R. Pastor-Satorras, C. Castellano, P. Van Mieghem, and A. Vespignani, *Rev. Mod. Phys.*, **87**(3), 925 (2015).  
[8] A. Barrat, M. Barthelemy, and A. Vespignani, *Dynamical processes on complex networks*. (Cambridge University Press, Cambridge, England, 2008).  
[9] W. Wang, M. Tang, H. E. Stanley, and L. A. Braunstein, *Rep. Prog. Phys.*, **80**(3), 036603 (2017).  
[10] C. Liu, X. X. Zhan, Z.-K. Zhang, G. Q. Sun, and P. M. Hui, *New J. Phys.* **17**(11), 113045 (2015).  
[11] Z.-K. Zhang, C. Liu, X. X. Zhan, X. Lu, C. X. Zhang, and Y. C. Zhang, *Phys. Rep.* **651**, 1-34 (2016).  
[12] Y. Y. Chen, F. Chen, D. Gunnell, and P. S. F. Yip, *PloS One* **8**, e55000 (2013).  
[13] Y. C. Zhang, S. Zhou, Z. Z. Zhang, J. H. Guan, and S. G. Zhou, *Phys. Rev. E* **87**, 032133(2013).  
[14] Y. Moreno, M. Nekovee, and A. F. Pacheco, *Phys. Rev. E* **69**, 066130 (2004).  
[15] A. Montanari, and A. Saberi, *Proc. Natl Acad. Sci. USA* **107**, 20196C201 (2010).  
[16] R. Peres, *Physica A* **402**, 330C43 (2014).  
[17] D. Centola, *Science* **329**, 1194 (2010).  
[18] M. Zheng, L. Lü, and M. Zhao, *Phys. Rev. E* **88**(1), 012818 (2013).  
[19] D. Blansky, C. Kavanaugh, C. Boothroyd, B. Benson, J. Gallagher, J. Endress, and H. Sayama, *PLoS One* **8**, e55944 (2013)

- [20] J. Allen, M. Weinrich, W. Hoppitt, and L. Rendell, *Science* **340**, 485C8 (2013)
- [21] B. Dybiec, N. Mitarai, and K. Sneppen, *Phys. Rev. E* **85**, 056116 (2012)
- [22] A. Nematzadeh, E. Ferrara, A. Flammini, and Y. Y. Ahn, *Phys. Rev. Lett.* **113** 088701 (2014)
- [23] K. Nagata, and S. Shirayama, *Physica A* **391**, 3783C91 (2012).
- [24] W. Wang, M. Tang, H. F. Zhang, and Y. C. Lai, *Phys. Rev. E* **92**, 012820 (2015).
- [25] Y. X. Zhu, W. Wang, M. Tang, and Y. Y. Ahn, *Phys. Rev. E* **96**(1), 012306 (2017).
- [26] P. L. Prapivsky, S. Redner, and D. Volovik, *J. STAT. MECH.-THEORY E.*, **2011**(12), P12003 (2011).
- [27] D. J. Watts, and S. H. Strogatz, *Nature* **393**, 440 (1998)
- [28] F. J. Pérez-Reche, J. J. Ludlam, S. N. Taraskin, and C. A. Gilligan, *Phys. Rev. Lett.* **106**, 218701 (2011).
- [29] F. C. Santos, J. F. Rodrigues, and J. M. Pacheco, *Phys. Rev. E* **72**, 056128 (2005).
- [30] S. Maslov, and K. Sneppen, *Science* **296** 910 (2002).
- [31] C. Castellano, S. Fortunato, and V. Loreto, *Rev. Mod. Phys.* **81**, 591 (2009).
- [32] M. E. J. Newman, *SIAM Rev.* **45**, 167 (2003).
- [33] R. Pastor-Satorras, and A. Vespignani, *Phys. Rev. Lett.* **86** 3200 (2001).
- [34] J. Zhou, Z. Liu, and B. Li, *Phys. Lett. A* **368** 458 (2007).
- [35] A. Sudbury, *J. Appl. Prob.* **22**, 443(1985).
- [36] D. H. Zanette, *Phys. Rev. E* **64**, 050901(R) (2001).
- [37] D. H. Zanette, *Phys. Rev. E* **65**, 041908 (2002).
- [38] Z. Liu, Y.-C. Lai, N. Ye, *Phys. Rev. E* **67**, 031911 (2003).
- [39] S. Goel, D. J. Watts, and D. J. Goldstein, *Proc. 13th Int. Conf. EC (New York: ACM)* pp 623C38 (2012).
- [40] J. L. Iribarren and E. Moro, *Phys. Rev. Lett.* **103**, 038702 (2009).
- [41] J. L. Iribarren and E. Moro, *Phys. Rev. E* **84**, 046116 (2011).
- [42] S. N. Majumdar and P. L. Krapivsky, *Phys. Rev. E* **63**, 045101(R) (2001).
- [43] H. P. Young, *Amer. Econ. Rev.* **99**, 1899 (2009).
- [44] C. de Kerchove, G. Krings, R. Lambiotte, P. Van Dooren, and V. D. Blondel, *Phys. Rev. E* **79**, 016114 (2009).
- [45] B. Karrer and M. E. J. Newman, *Phys. Rev. E* **82**, 016101 (2010).
- [46] J.-P. Onnela and F. Reed-Tsochas, *Proc. Natl. Acad. Sci. U.S.A.* **107**, 18375 (2010).
- [47] L. Lü, D.-B. Chen, T. Zhou, *New J. Phys.* **13**, 123005 (2011).
- [48] J. Gómez-Gardeñes, L. Lotero, S. N. Taraskin and F. J. Pérez-Reche, *Sci. Rep.* **6**, 19767 (2016).
- [49] Q. H. Liu, W. Wang, M. Tang, T. Zhou, and Y. C. Lai, *Phys. Rev. E* **95**(4), 042320 (2017).
- [50] P. S. Dodds and D. J. Watts, *Phys. Rev. Lett.* **92**, 218701 (2004).
- [51] P. S. Dodds and D. J. Watts, *J. Theor. Biol.* **232**, 587 (2005)
- [52] K. Chung, Y. Baek, D. Kim, M. Ha, and H. Jeong, *Phys. Rev. E* **89**, 052811 (2014).
- [53] Y. Sano, K. Yamada, H. Watanabe, H. Takayasu, and M. Takayasu, *Phys. Rev. E* **87**, 012805 (2013).
- [54] F. Wu, and B. A. Huberman, *Proc. Natl Acad. Sci. USA* **104**, 17599 (2007)
- [55] D. J. Watts, *Proc. Natl. Acad. Sci. USA* **99**, 5766 (2002).
- [56] L. Lü, D. Chen, X. L. Ren, Q. M. Zhang, Y. C. Zhang, and T. Zhou, *Phys. Rep.* **650**, 1-63 (2016).
- [57] E. Volz, *J. Math. Biol.* **56**(3), 293-310 (2008).
- [58] J. C. Miller, *J. Math. Biol.* **62**(3), 349-358 (2011).
- [59] P. Shu, W. Wang, M. Tang, P. Zhao, and Y. C. Zhang, *Chaos* **26**(6), 063108 (2016).
- [60] J. C. Miller, A. C. Slim, and E. M. Volz, *J. R. Soc. Interface* **9**(70), 890-906 (2012).
- [61] J. C. Miller, and E. M. Volz, *PLoS One* **8**(8), e69162 (2013).
- [62] J. C. Miller, *PLoS one* **9**(7), e101421 (2014).
- [63] W. Wang, M. Tang, P.-P. Shu, and Z. Wang, *New J. Phys.* **18**, 013029 (2015).
- [64] S. H. Strogatz, *Nonlinear Dynamics and Chaos: With Applications to Physics, Biology, Chemistry, and Engineering (Studies in Nonlinearity)*, 2nd ed. (Westview Press, Colorado, USA, 2014).
- [65] M. A. Serrano and M. Boguñá, *Phys. Rev. Lett.* **97**, 088701 (2006).
- [66] M. E. J. Newman, *Phys. Rev. Lett.* **103**, 058701 (2009).
- [67] M. Girvan and M. E. Newman, *Proc. Natl. Acad. Sci. USA* **99**, 7821 (2002).
- [68] S. Fortunato, *Phys. Rep.* **486**, 75 (2010).
- [69] K. Gong, M. Tang, P. M. Hui, H. F. Zhang, Y. Do, and Y.-C. Lai, *PLoS ONE* **8**, e83489 (2013).
- [70] S. P. Borgatti and M. G. Everett, *Soc. Net.* **21**, 375 (2000).
- [71] P. Holme, *Phys. Rev. E* **72**, 046111 (2005).
- [72] Y. Liu, M. Tang, T. Zhou, and Y. Do, *Sci. Rep.* **5**, 9602 (2015).
- [73] T. Verma, F. Russmann, N. Araújo, J. Nagler, and H. Herrmann, *Nat. Commun.* **7**, 10441 (2016).
- [74] S. Boccaletti, *et al.* *Phys. Rep.* **544**, 1 (2014)
- [75] C.-G. Gu, S.-R. Zou, X.-L. Xu, Y.-Q. Qu, Y.-M. Jiang, D.-R. He, H.-K. Liu, and T. Zhou, *Phys. Rev. E* **84**, 026101 (2011).
- [76] M. Zheng, M. Zhao, B. Min, and Z. Liu, *Sci. Rep.*, **7**, 2424 (2017)
- [77] P. Holme and J. Saramäki, *Phys. Rep.* **519**, 97 (2012).